Seismic monitoring of Kangding Ms6.3 earthquake on the slope response

Wang Yunsheng(1), He Jianxian(2), Luo Yonghong(1), Cao Shuihe(2), He Zihao(2)

(1) State Key Lab. of Geo-Hazard Prevention and Geo-Environment Protection,
Chengdu University of Technology, China
(2) College of Environment and Civil Engineering, Chengdu University of Technology, China

Abstract

Some earthquakes whose magnitude is lower than Ms 7.0 induced strong secondary geohazards such as Ludian earthquake of Yunnan in 2014 and Qianjiang earthquake of Chongqing in 1856, topographic amplification is considered to be the main factor for the slope failure. However, up to now, seismic monitoring data are not enough to support the idea. Kangding Ms 6.3 earthquake on November 22, 2014 was monitored in Lengzhuguan section, Sichuan, China. Six monitoring instruments in the slope adits were triggered by the earthquake. The data reveals: (1) compared with the valley bottom reference point of Guza station, the horizontal PGA amplification factors of #1 station at the top of the ridge on the right bank is 10.6-11.5, and the vertical one is 7.1; and the Arias Intensity is also significantly stronger; the horizontal PGA amplification factor of #2 station at the middle part on the right bank is 4.3-5.0, and the vertical one is 2.3; (2) the PGA amplification factors of the stations on the left bank are smaller than those of the right bank and only PGA amplification factor at the slope break is higher: the horizontal PGA amplification factor of #5 at the slope break is higher, from 3.0-4.5, and the vertical one is 2.3, the horizontal PGA amplification factor of #6 range from 1.9 to 2.1, and the vertical one is 1.7; (3) the outer part PGA amplification factor of #7 station is larger than that of the inner part; (4) Horizontal to vertical spectral ratio illustrates that the #1 station on the right topographic amplification factor of horizontal component reaches 11.1, and Predominant period is concentrated in the low-frequency on the right bank; while there are several Predominant period on the left bank and the amplification effect is more prominent at high-frequency.

Key words: Kangding Ms6.3 earthquake, topography amplification effect, Lengzhuguan section, slope seismic response

1. Introduction

Since last century, based on geological survey on the slope seismic response and theoretical model calculation, scholars at home and abroad have found that there are topographic amplification effects at protruding topography, slope break and butte under strong earthquake, where more slope failures happened than other parts of the slope on the whole. The seismic response data analysis of Central Chile earthquake in 1985 revealed that the frequency range of ground motion amplification can be obtained by the frequency ratio method and the amplification effects was obvious at special geological site and mountain ridge (Celebi, 1987). Geli (1988) revealed the topographic amplification effects are obvious at the top of the hill where slope width is approximately equal to the incident wavelength; incident P-wave topographic amplification effect is lower than the incident S-wave; P-SV wave topographic amplification effect is slightly stronger than the SH wave; and topographic amplification effect would increase while the adjacent ridges exist. The mountain hazard survey of Wenchuan earthquake revealed that (Luo et al., 2013): the horizontal components of the seismic waves can be significantly enlarged by coupling of the terrain size and the seismic wavelength, and the amplification effect is distinct at the thin mountain ridge or bar mountain, the part of slope break, convexity slope. It can be concluded from Lushan earthquake mountain hazards (Huang et al., 2013): the source of rock fall is at upper part of the steep slope and prominent spur. Analysis of the Lengzhuguan slope of Lushan earthquake seismic response revealed that ground motion topographic amplification effect at thin ridge of the right bank was significantly stronger than the left bank of the alpine slopes (Luo et al., 2013). The higher peak ground acceleration records in Wenchuan earthquake were caused by the local topographic effects (Wen et al., 2013). Qi et al. (2007) simulated three-components of acceleration distribution. Based on surveying lots of secondary natural geological disasters caused by Lushan (2013) and Ludian (2014) earthquake (both magnitude were not high), some scholars thought it might be associated with topographic amplification effects, but it was still lack of a large number of monitoring data on the slope seismic response.

With the support of China Geological Survey Bureau (12120113009700), National Science Foundation of China (41072231), we set up a monitoring section in Lengzhuguan in 2011. At 16:55 of November 22th, 2014, a magnitude Ms 6.3 earthquake occurred in the Kangding County, Sichuan, China. The six seismic instruments were triggered in the section, a series of data reveals the topographic amplification discipline.

2. Summary of the monitoring profile

Lengzhuguan earthquake monitoring section is located in both sides of Lengzhuguan valley where the valley meets the Dadu River and the section is on the right bank of the Dadu River (Fig. 1). Seven stations are set in the section where two stations are on the right bank and five stations are on the left bank of Lengzhuguan valley. One seismic monitoring instrument is set in each station (the first to sixth station), and two monitoring instruments are set in the seventh station (outer is 57m from the portal and inner is 135m from the portal). The E-catcher strong motion seismographs made by Application of Japan earthquake measuring strain, and the basic parameters are sensitivity is 1V/G, metre full scale is 2000gal(1gal=1cm·s^{-2}), and the range of cycle frequency is DC~20Hz(-3dB).

3. Slope seismic response in Lengzhuguan section

The distances between the Kangding Ms 6.3 earthquake epicenter and the monitoring site is about 56km and the depth of hypocenter is 18 kilometers, and six strong monitoring instruments were triggered in the event. The parameters of the monitoring stations are shown in Table 1, and the waveform of monitoring stations (see Fig. 2) and the ground motion parameter characteristics of each monitoring station are listed in Table 2.

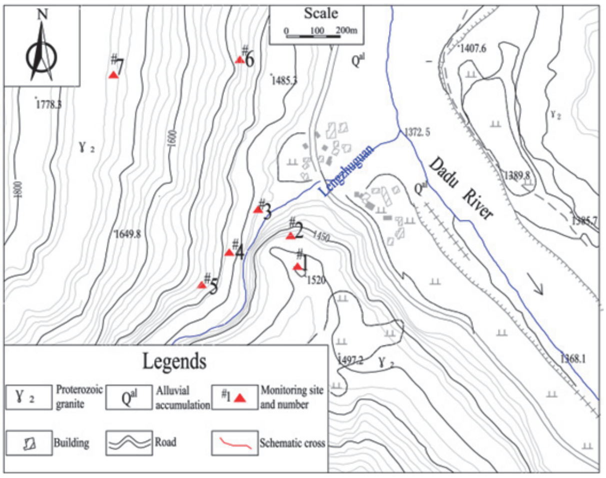

Fig. 1 The plane distribution map of Lenzhuguan slope seismic monitoring station

Table 1 The parameters of the monitoring stations

Number of monitoring stations	Elevation (m)	Epicentral distance (km)	Horizontal depths to portal(m)	Type of bed rock
#1	1516	56.2563	8	granite
#2	1478	56.2331	1	granite
#5	1518	56.0337	7	granite
#6	1520	55.9515	10	granite
#7(Outer)	1686	55.7189	57	granite
#7(Inner)	1686	55.7189	135	granite

Table 2 The ground motion parameter characteristics of the monitoring stations

Number of monitoring stations	PGA/(gal)			Arias intensity /(cm·s^{-1})			Dominant frequency /Hz		
	EW	SN	UD	EW	SN	UD	EW	SN	UD
#1	188.1	147.6	111.8	24.7	25.5	6.0	2.04	2.54	5.07
#2	70.4	69.9	36.5	2.4	2.3	0.6	2.04	2.04	5.31
#5	49.9	62.4	36.6	1.7	1.6	0.8	4.42	3.31	9.29
#6	35	26.4	27.6	0.5	0.3	0.3	1.24	1.01	8.59
#7(Outer)	24.9	22.7	14.0	0.3	0.3	0.2	1.26	1.02	1.19
#7(Inner)	22.5	19.8	12.0	0.3	0.3	0.1	1.24	1.01	1.17

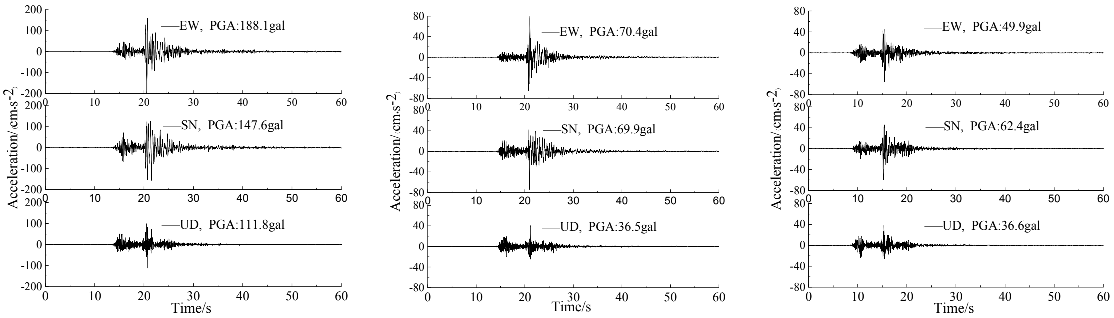

a. waveform of #1 station b. waveform of #2 station c. waveform of #5 station

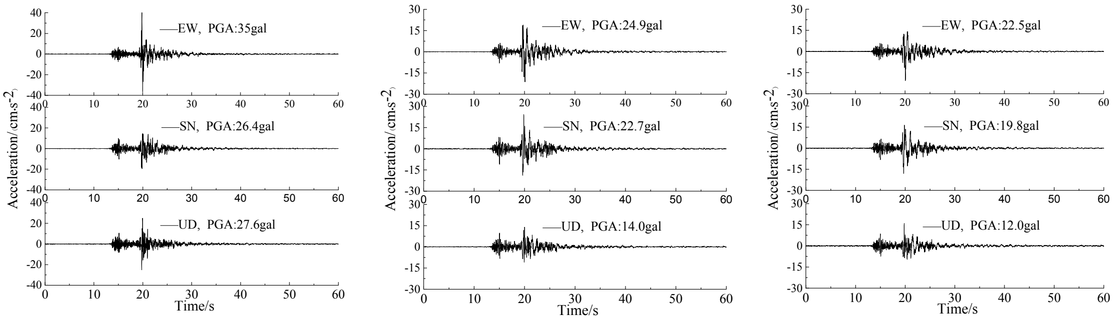

d. waveform of #6 station e. waveform of #7 station(outer) f. waveform of #7 station(inner)

Fig. 2 The acceleration waveform of monitoring stations

According to the seismic data of #1, #2, #5, #6 station and the outside and inside of #7 station, the horizontal and vertical component PGA of #1 station is 188.1gal and 111.8gal respectively, and the horizontal and vertical component PGA of inside monitoring instrument of #7 station are 22.5gal and 12.0gal respectively. The horizontal and vertical component PGA of #5 station is 62.4gal and 36.6gal on the left bank. The data reveals that the PGA on the right bank is about three times as those on the left. The PGA of the outside of #7 station (57m from the adit portal) monitoring station is larger than the inside (135m from the adit portal).

Site response directivity can be effectively analyzed by examining directional variation of Arias intensity (Arias, 1970). The Arias intensity (Ia) in three directions of each monitoring station are shown in Table 2, from which the horizontal and vertical Ia of #1 station are 25.5 and 6.0cm/s, and the horizontal and vertical Ia of #5 station are 1.7 and 0.8cm/s on the left bank. The maximum horizontal Ia on right bank is about 15 times as much as that on the left bank and the vertical Ia is about 7.5 times. We can also find that the horizontal and vertical Ia of #1 are about 2.7 and 3.1 times as much as that of #2 on the right bank, and the #6 are about 1.4 and 2.0 times as much as that of #7, and the outer and inner Ia of #7 is at the same level. Therefore, the seismic energy of the right bank is stronger than that of the left bank.

Table 2 reveals the horizontal predominant frequency of #1 and #2 station on the right bank is about 2.04 to 2.54 Hz and the vertical is 5.07 to 5.31 Hz. And the EW predominant frequency of #5 station is 4.42 Hz, SN is 3.31 Hz, and the vertical is 9.29 Hz. The EW and SN predominant frequency of #6 station are 1.24 and 1.01 Hz, and the vertical is about 8.59 Hz. The outer and inner predominant frequencies of #7 monitoring station are same: the east to west predominant frequency is 1.24 Hz, south to north is 1.01 Hz, and the vertical is 1.17 Hz.

4. The acceleration response spectrum

The concept of the response spectrum was carried out based on Elastic system dynamics (M. A. Biot, 1941). Later a series of response spectrum curve were obtained by some typical strong earthquake accelerations (G.W.Housner, 1959). Response spectrum is defined as the relationship between absolute value of the maximum response with cycle which is at the same damping ratio of a series of single degree of freedom system, and its essence is the reaction of ground motion characteristics. According to Chinese Specification of Strong Motion Safety Monitoring for Hydraulic Structures (DL/T 5416-2009), the horizontal and vertical acceleration response spectrum which are in different damping ratio (for 0.05, 0.1, 0.2) are calculated (see Fig. 3).

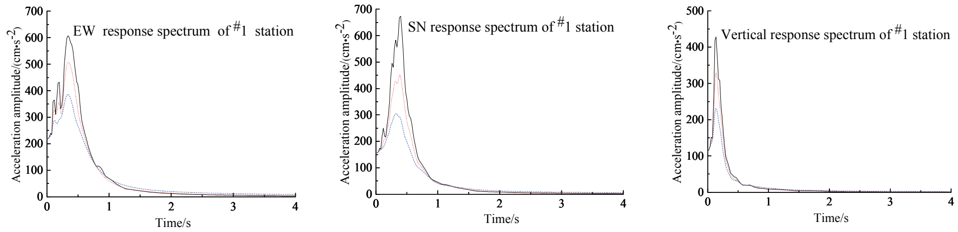

a. the acceleration response spectrum of #1 station

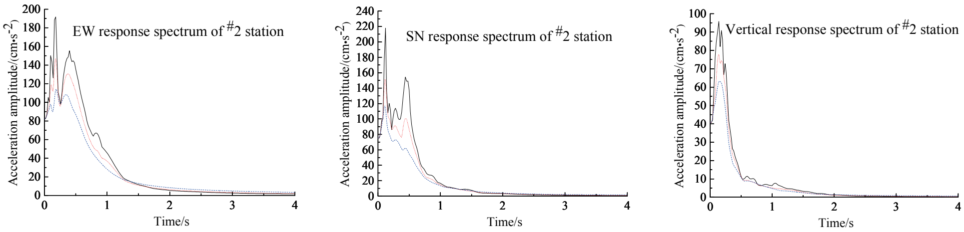

b. the acceleration response spectrum of #2 station

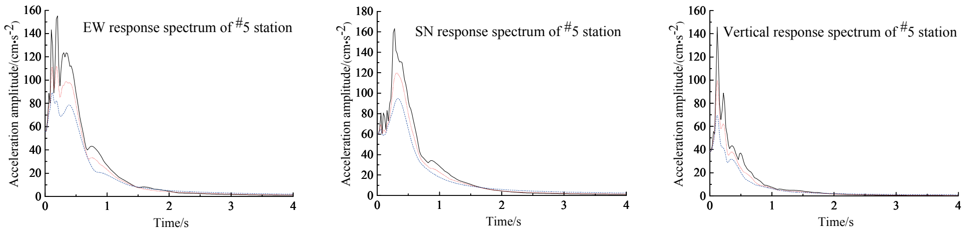

c. the acceleration response spectrum of #5 station

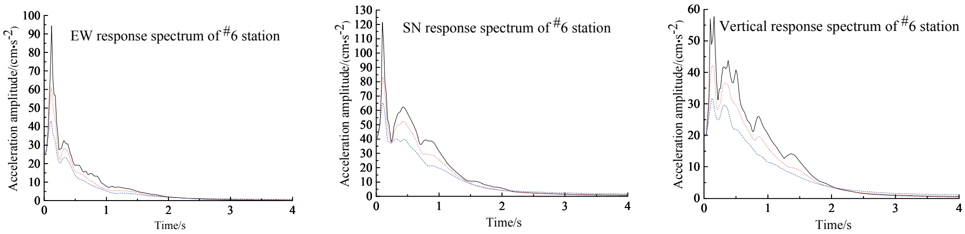

d. the acceleration response spectrum of #6 station

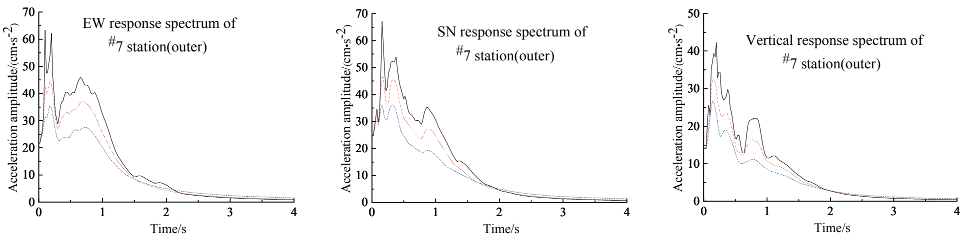

e. the acceleration response spectrum of #7 station(outer)

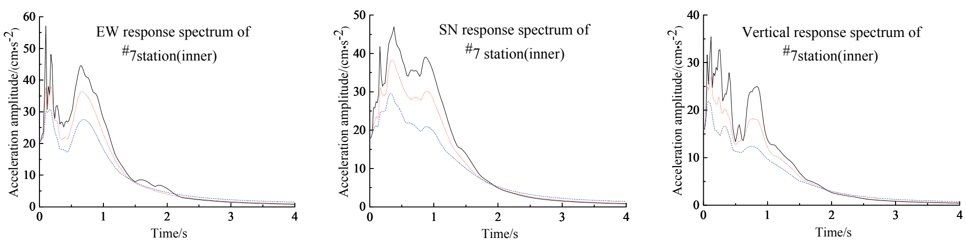

f. the acceleration response spectrum of #7 station(inner)

Damping ratio of 5%, Damping ratio of 10%, Damping ratio of 20%

Fig. 3 The acceleration response spectrum of monitoring stations

The acceleration amplitude decreased with the increasing of damping ratio, and the acceleration amplitude is at the largest with the damping ratio of 0.05. The ups and downs of horizontal or vertical acceleration response spectrum curve of each monitoring point are more consistent, i.e., obtaining the acceleration amplitude in different damping ratio at the same time. The results show that the seismic amplitude value is affected by the damping characteristics of ground while the process of ground motion characteristics is not affected obviously. The horizontal acceleration amplitude of each monitoring point is bigger than the vertical with various damping ratio which is consistent with the waveform of monitoring stations. Compared with the acceleration response spectrum curve of $^{\#}$1 and $^{\#}$2 station on the right bank, the horizontal acceleration amplitude of $^{\#}$1is about 3.1 times as the $^{\#}$2 station with the same damping ratio, and the vertical is up to 4.5. What's more, the acceleration amplitude of $^{\#}$1 station with the damping ratio of 0.2 is also bigger than the $^{\#}$2 station which damping ratio is 0.05, which is also bigger than each monitoring stations on the left bank with the damping ratio of 0.05. So the acceleration amplitude of response spectrum on the right bank is bigger than that on the left bank.

5. Topography amplification effect

Reference to Guza strong earthquake monitoring station of the main shock records (its horizontal and vertical component PGA was16.4 and 15.7gal) which is about 7 km apart from the Lengzhuguan monitoring section, the PGA amplification coefficients of each monitoring stations are shown on the Fig. 4.

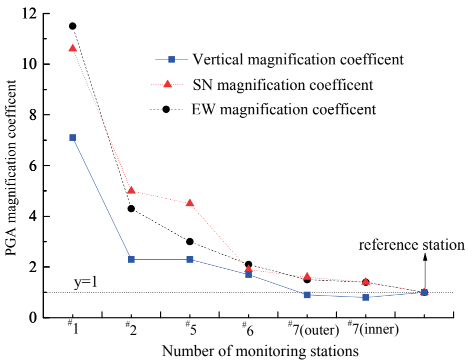

Fig. 4 The PGA response coefficient of each monitoring station

Fig. 4 show that the EW PGA amplification coefficient of $^{\#}$1 station is 11.5 and the vertical PGA magnification coefficient is 7.1, while both of $^{\#}$2 station are 5.0 and 2.3; and the horizontal and vertical PGA amplification coefficient of $^{\#}$5 station is about 4.4 and 2.3; the horizontal PGA amplification coefficient of $^{\#}$6 is about 2.1 and the vertical is merely 1.7; the outer and inner horizontal PGA amplification coefficient of $^{\#}$7 station is between 1.3 and 1.6, however the vertical PGA magnification coefficient is decreased partly. So the PGA amplification on the right bank is much larger than the left, and the $^{\#}$1 is larger than $^{\#}$2 station on the right bank, and the $^{\#}$5 is larger than $^{\#}$6 and $^{\#}$7 station on the left bank.

6. Conclusion

Reference to Guza station of the main shock record of Kangding Ms6.3 earthquake (its horizontal and vertical component PGA was16.4 and 15.7gal), the monitoring data on the two bank of Lengzhuguan section reveals obvious topography amplification effects: (1) the horizontal and vertical PGA amplification coefficients of $^{\#}$1 station which is on the top of the peninsular terrain on the right bank reach 10.6-11.5 and 7.1; (2)$^{\#}$2 monitoring station is 4.3-5.0 and 2.3; (3)the horizontal and vertical PGA amplification coefficients of $^{\#}$5 station which is on the left nearly linear slope is 3.0-4.5 and 2.3; (4) $^{\#}$6 station is 1.9-2.1 and 1.7; (5)horizontal PGA amplification coefficients of $^{\#}$7 station is1.46-1.6.

Acknowledgements

This study is financially supported by the National Foundation for Natural Science of China (41072231) and the foundation of China Geological Survey (12120113009700).

Reference

[1] Celebi. Topographic and geological amplification determined from strong motion and aftershock records of March 1985 Chile earthquake [J]. Bull. Seis. Soc. Am 1987, 77: 1147-1167.

[2] Geli L, Bard P Y, Jullien B. The effect of topography on earthquake ground motion: a review and new results [J]. Bull. Seism. Soc. A. 1988, 78:42-63.

[3] Luo Yonghong, Wang Yunsheng. A study on the mountain slope ground motion topography amplification effect induced by Wenchuan Earthquake. Journal of Mountain Science, 2013, 31(2):200-210.

[4] Huang Runqiu, Wang Yunsheng, Pei Xiangjun, et al. Characteristics of Co-seismic Landslides Triggered by the Lushan Ms7.0 Earthquake on the 20th of April, Sichuan Province, China[J]. Journal of Southwest Jiao Tong University, 2013, 48(4):581-589.

[5] Luo Yonghong, Wang Yunsheng, He Yuan, et al. Monitoring result analysis of Lenzhuguan slope

ground shock response of Lushan earthquake of Sichuan,China[J]. Journal of Cheng Du University of Technology (Science &Technology Edition), 2013,40(3):232-241.

[6] Wen Ruizhi, Ren Yefei, Qi Wenhao, et al. Maximum Acceleration Recording from Lushan Earthquake on April 20, 2013[J]. Journal of Southwest Jiao Tong University, 48(5):783-791.

[7] Chen Guoping, Wen Liuhan·Heisha, Wang Shuai. Comparisons of various characteristic parameters of strong motions[J]. South China Journal of seismology, 2011,31(2):45-54.

[8] Boit MA. A Mechanical Analyzer for Prediction of Earthquake Stress[J]. Bull.Seism.Soc. Am, 1941, 31: 151-171.

[9] Housner GW. Behavior of Structures during Earthquakes[J]. ASCE, 1959, 85(EM4): 109-129.

[10] Chavez Garcia F J, Dominguez T, Rodriguez M, et al. Site effects in a volcanic environment: a comparison between HVSR and array techniques at Colima, Mexico[J]. BSSA, 2007, 97 (2) : 591-604.

[1 1] Xu Qiang, Li Weile. Study on the Direction Effects of Landslides Triggered by Wenchuan Earthquake[J]. Journal of Si Chuan University (Engineering Science Edition, 2010, 42(Supp.2):7-14.

[1 2] Arias, A, 1970. A Measure of Earthquake Intensity in Seismic Design for Nuclear Power Plants. MIT Press, Cambridge, Mass, pp. 438–483.